Kobe University Repository : Kernel

PDF issue: 2025-12-05

Effects of texture and stress sequence on twinning, detwinning and fatigue crack initiation in extruded magnesium alloy AZ31

Nakai, Yoshikazu
Kikuchi, Shoichi
Asayama, Kaito
Yoshida, Hayata

(Citation)
Materials Science and Engineering: A,826:141941

(Issue Date)
2021-10-05

(Resource Type)
journal article

(Version)
Accepted Manuscript

(Rights)
© 2021 Elsevier B.V.
This manuscript version is made available under the Creative Commons Attribution-NonCommercial-NoDerivatives 4.0 International license.

(URL)
https://hdl.handle.net/20.500.14094/90008614

KOBE UNIVERSITY

Revised Manuscript - clean version
Click here to view linked References

Effects of Texture and Stress Sequence on Twinning, Detwinning and Fatigue Crack Initiation in Extruded Magnesium Alloy AZ31

Yoshikazu Nakai
Department of Mechanical Engineering, Kobe University, Nada, Kobe 657-8501, Japan
nakai@mech.kobe-u.ac.jp
Corresponding author

Shoichi Kikuchi
Department of Mechanical Engineering, Shizuoka University, Naka, Hamamatsu 432-8561, Japan
kikuchi.shoichi@shizuoka.ac.jp

Kaito Asayama
Department of Mechanical Engineering, Kobe University, Nada, Kobe 657-8501, Japan
kaito.mln0928@gmail.com

Hayata Yoshida
Department of Mechanical Engineering, Kobe University, Nada, Kobe 657-8501, Japan
big.peregrine@gmail.com

Keywords: Compression–compression fatigue; Crack formation; High cycle fatigue; Magnesium alloy; Twinning–detwinning

Submitted for the publication of Materials Science and Engineering: A

Abstract

Several types of cyclic stress were applied to specimens made of an extruded magnesium alloy, AZ31, to elucidate twinning, detwinning, and fatigue crack initiation mechanisms by electron backscattered diffraction analysis. In both the texture and the random orientation, twinning occurred under compressive stress exceeding the compressive yield strength. Detwinning occurred only in the texture upon the subsequent application of tensile stress less than the tensile yield strength of monotonic loading, whereas detwinning did not occur in the structure with random orientation. Under compression–compression fatigue test, successive twinning occurred, which changed the orientation of the basal plane. As a result, the random orientation of grains changed to the texture in which the normal of the basal plane was parallel to the loading direction. Cracks were formed along the boundary of grains with a high Schmid factor of the basal slip system and the misfit of grain on both sides was large. Near the crack initiation site, twin bands were observed; however, detwinning did not occur under the tensile stress after the cyclic compression loading.

1. Introduction

Recently, magnesium alloys have been receiving considerable attention because of their high specific strength, which is especially important in mobile devices and transportation systems. Therefore, their mechanical properties and mechanisms of deformation and fracture should be understood.

It is well known that twinning plays an important role in the compressive plastic deformation of magnesium alloys with the hcp crystal structure, the slip system of which is limited. Then, the twinning is important to understand the cold working process in which all grains are subjected to plastic deformation. Meanwhile, the twin bands formed under compressive stress sometimes disappear after the following application of tensile stress, which is called detwinning [1-5]. This phenomenon has been related with fatigue crack initiation, which is one of the most important mechanical properties to pay attention to regarding the long use of transportation systems. The twinning–detwinning behavior in most of the previous studies has been examined by monitoring the evolution of X-ray diffraction peaks, which reveals all the behaviors of several grains in the observation area, although fatigue crack initiation is a localized phenomenon limited to a grain or a grain boundary. To investigate the fatigue crack initiation behavior, successive observations should

be conducted at the crack initiation site over a number of cycles. Furthermore, the previous studies have been conducted under fully reversed low-cycle fatigue conditions, and the crack initiation mechanism under compression–compression fatigue, where detwinning should not occur, has not yet been clarified.

Murphy-Leonard et al. [6] studied the cyclic twinning and detwinning behaviors of an extruded magnesium alloy under fully reversed low-cycle fatigue conditions, and twinning and detwinning behaviors were characterized by monitoring the evolution of X-ray diffraction peaks. They found that twinning occurs during the compression portion of the cycle at the early stages of fatigue, and most twins are detwinned under reversed loading during the tensile portion of the cycle. They also observed that the detwinning process was incomplete after 100–200 fatigue cycles, and a significant fraction of residual twins remained throughout one entire cycle. They concluded that the increase in the number of residual twins corresponds to fatigue damage. They also observed persistent twinning by electron backscattered diffraction (EBSD); however, it has not yet been clarified whether the twinning–detwinning phenomenon occurs in each cyclic loading or whether the fatigue crack initiation is affected by such a phenomenon.

The role of twinning and detwinning in the fatigue process depends on the extent of plastic deformation. For example, in the low-cycle-fatigue regime, where all grains deform plastically as in cold working, fatigue cracks are usually initiated from the twin boundaries in polycrystalline magnesium alloys without defects or inclusions [7-9]. In the high-cycle-fatigue regime, however, it has been observed for conventional alloys that plastic deformation occurs only in some grains [10-12] without macroscopic plastic deformation. Actually, it has been reported by Shiozawa et al. [7] that the fatigue crack initiation mechanism is the twin-induced failure mode at high stress amplitudes and the slip-induced failure mode at low stress amplitudes. Murphy-Leonard et al. [6] also reported that, for low-cycle fatigue, twinning and detwinning were observed at a high strain amplitude but not at a low strain amplitude. Thus, twinning may not always be required for fatigue crack initiation in magnesium alloys. However, it is still unclear whether twinning is involved in crack initiation in the high-cycle-fatigue regime [7,9,13,-22].

The authors conducted fatigue tests under several stress ratios with positive mean stress and fully reversed cyclic loading to elucidate the fatigue crack initiation mechanism in an extruded magnesium alloy, AZ31, and the specimen surface near the crack initiation site was analyzed by EBSD to

elucidate the fatigue crack initiation mechanism [4,5]. They concluded that fatigue cracks are not formed from twin bands but from large grains with a high Schmid factor of the basal slip system, and that the crack initiation mechanism is a result of irreversible slipping and is unrelated to twinning under fully reversed cyclic stress (R=–1).

The effects of the crystallographic orientation, *i.e.*, random orientation vs crystallographic texture, on twinning and detwinning in magnesium alloys also have not yet been clarified. Cold rolling magnesium alloy usually has a texture [23] in which the *c*-axis (the normal of the basal plane) in most grains is perpendicular to the extruded direction, and the mechanical and fatigue tests are usually conducted with force applied in the extruded direction. As described later, we found that the orientations of grains very near the surface of the extruded plate are randomly distributed, and we could examine the effect of the difference between grains with texture and random distribution on twinning, detwinning, and fatigue crack initiation behaviors.

In this study, the EBSD analysis was conducted to clarify factors affecting twinning, detwinning, and fatigue crack initiation behaviors employing different microstructures and loading patterns, including compression–compression fatigue. By comparison with our previous results of fully reversed loading fatigue, the differences in the twinning and crack initiation behaviors are discussed.

2. Material and Experimental Procedures

2.1 Material and specimen

The material for this study was an extruded AZ31 magnesium alloy plate. The chemical composition (in mass %), the average grain size, and the mechanical properties of the alloy are shown in Tables 1 and 2, respectively. As shown in Table 2, the yield strength under compression is much lower than that under tension because of the twinning under compression. The results of the EBSD analysis around the midsection, and side surface of the as-received plate are shown in Fig. 1 and Fig. 2 (c), respectively, where colors indicate orientation of each grain. Figure 2 (c) indicates that the as-received plate has crystallographic texture whose *c*-axis ({0001} direction, shown by red) in most grains is perpendicular to the extruded direction (L-direction) at a depth from the surface greater than 0.3 mm, while the crystallographic orientation is random near the surface. Philippe reported that the extent of texture is changed with the distance from the surface in rolled magnesium plate [24].

Specimens with the dimensions shown in Figs. 3 (a) and (b) were cut from the extruded plate of 3.2 mm thickness as shown in Figs. 3 (c) - (e), where the grains at the surfaces of Type A have crystallographic texture as shown in Fig. 2 (b), and the orientation of grains at the surface of Type B and Type C specimens are random as shown in Fig 2 (a). Type A and Type B specimens were employed for the observations of the initial few cycles, and Type C specimen for compression–compression (stress ratio: R=10) fatigue tests, respectively, where the longitudinal (loading) direction of the specimen coincided with the extruded direction. The stress concentration factor K_t of Type A and Type B specimens are 1.05, and it is 1.01 for Type C specimen [25]. Since the fatigue notch factor K_f is almost equal to K_t, for $K_t < 2$ [26], the fatigue strength of these specimens can be determined by the stress state at the notch root regardless to the notch root radius and the geometry of the cross-section.

2.2 Fatigue test

For compression–compression fatigue tests, the sinusoidal loading wave with the frequency of 30 Hz was employed using an electrodynamic vibrator driven by a power supply under the current-controlled mode as shown in Fig. 4. This system was controlled by a personal computer to maintain the amplitude and mean value of the applied force constant. The four-point bending moment was applied to specimens through a loading device shown in Fig. 5, where the distances between the inner and outer pins were 5.0 mm and 15.0 mm, respectively. Although plane bending test is useful to examine the mechanical and fatigue properties of surface layer of samples, the tensile stress and the compressive stress always appeared simultaneously in both sides of the neutral axis of specimen, and cracks always initiate and propagate from the tensile mean stress side for specimens with a symmetrical cross-section, such as a rectangle, where the absolute value of the compressive stress is equal to the tensile stress. However, the ratio of the compressive stress to the tensile stress at the surface is not equal for specimens with non-symmetrically shaped cross-section. In this study, a T-shaped cross-sectional plate was employed to control the ratio of the compressive stress to the tensile stress. For the specimen with the dimensions of cross-section shown in Fig.3 (b), the ratio of the maximum absolute compressive stress to the maximum tensile stress is 3.0, which induces crack initiation in compression–compression fatigue test at a stress ratio R of 10. The maximum and minimum stress of fully reversed cyclic loading were 140 MPa and -140 MPa, and those of compression-compression fatigue were -14 MPa and -140 MPa, respectively.

The orientations of grains and the twinning and detwinning behaviors were observed by EBSD analysis. Although surface polishing was required just before the EBSD analyses to remove the surface oxidation layer, the conventional mechanical polishing introduces plastic deformation, which may cause twinning. Therefore, cross-sectional polishing by argon ion milling was performed to remove the surface oxidation layer [4].

3. Experimental Results

3.1 Fully reversed cyclic stress

The orientation of grains on the specimen surface after the start of cyclic loading with the tension for the Type A specimen which exhibits texture surface, is shown in Fig. 4. The observations were conducted (a) before the first loading, (b) at the time of unloading after the application of tensile stress, and (c) at the time of unloading after the following application of compressive stress, as schematically shown in upper side of the figure, where the maximum tensile stress was less than the tensile yield strength σ_{YT}, and the maximum compressive stress (absolute value) exceeded the compressive yield strength σ_{YC} under monotonic loading.

Note that these figures were obtained at the same site of a specimen, but the shape of grains are not exactly the same for every observation because the cross-sectional polishing was conducted to remove the surface oxidation layer for every EBSD analysis. In Figs. 4 show that (a) the specimen had no initial twin bands, and (b) twin bands were not formed under tensile stress, but (c) many $[10\bar{1}1]$ twin bands were formed under compressive stress, some of them are indicated by arrows. Since non-linear stress-strain relationship was observed only under compressive and tensile loading process, and it was linear under unloading process [4], twinning and detwinning must occurred under loading process. The orientation of grains on the specimen surface after the start of cyclic loading with compression for the Type A specimen, which has texture surface, is shown in Fig. 5. The EBSD analyses were conducted before the first loading (a), and at the time of unloading in (b), (c), and (d), where the maximum compressive stress (absolute value) exceeded the compressive yield strength σ_{YC}, and maximum tensile stress was less than the tensile yield strength σ_{YT} under monotonic loading. Figures 5 (b) and (d) were obtained after the unloading following application of compressive stress, where the bands indicated by arrows are the $[10\bar{1}1]$ twin bands, and (c) was obtained after unloading

following application of tensile stress, where all twin bands disappeared without the formation of new twin bands, which is similar to our previous observation [4].

The orientation of grains on the specimen surface after the start of cyclic loading with compression for Type B specimen, in which the orientation of grains at the surface is random, is shown in Fig. 6. The loading pattern is similar to that for Fig. 5. After the application of compressive stress, twin bands, indicated by downward arrows, were formed as shown in Fig. 6 (a), and after the following application of tensile stress, part of the twin bands formed under compressive stress, indicated by right-pointing arrows in (a), disappeared due to detwinning, but those indicated by downward arrows persist. Moreover, new $[10\bar{1}2]$ twin bands, shown by left-pointing arrows in (b), appeared in $[\bar{1}2\bar{1}0]$ plane under tensile stress, indicating that twin bands are formed not only under compressive stress but also under tensile stress in grains whose *c*-axis is parallel to the loading direction.

3.2 Twinning and crack initiation under compression–compression fatigue

In the previous section, the twinning and detwinning behaviors were observed at the start of cyclic loading. In this section, the change in the crystallographic structure after fatigue crack initiation was observed. Figure 7 shows the orientation of grains on the specimen surface after the cyclic loading of 1.0×10^7 cycles under the stress ratio $R = 10$ for Type C specimen with the random orientation of grains at the surface before the fatigue test, where the grain orientations indicate (a) perpendicular to the surface, (b) parallel to the loading direction, and (c) parallel to the transverse direction, respectively. At this number of cycles ($N = 1.0\times10^7$), fatigue cracks are already initiated but do not propagate. Figure 7 (a) are different from that shown in Fig. 2 (a), and similar to Fig. 2 (b), indicating that the direction of the *c*-axis in most of grains was rotated from S-direction to L-direction.

Figure 8 shows microscopies around the crack initiation site at $N = 1.0\times10^7$ cycles in compression–compression fatigue test ($R = 10$, $\sigma_a = 63$ MPa) using Type C specimen, which has the random orientation surface before the fatigue test, where (a) is the optical microscopy, (b) and (c) are the orientation of grains, and (d) is the Schmid factor, those were obtained by the EBSD analysis. Since it is difficult to distinguish between grain boundaries and cracks in the EBSD analysis, the crack was shown as the white line in Figs. 8 (b), (c), and (d). Figure 8 (b) shows that the crack initiated along grain boundaries with large misfit. One of the grains had high Schmid factor of the

basal slip system, as shown in Fig. 8 (d). Near the crack initiation site, twin bands, indicated by arrows, were formed; however, no twin bands can be observed at the crack initiation site. Therefore, the twin deformation must not have affected the crack initiation mechanism. After this observation, tensile stress was applied to the specimen and the EBSD analysis was conducted. Although detwinning occurs under tensile stress after twinning due to application of compressive stress as shown in Fig. 5, Fig. 8 (c) shows that the detwinning under tensile stress after compression–compression fatigue test did not occur similar to the case shown in Fig. 6.

Results shown in Figs. 4-8 indicate that the detwinning mechanism applies only to grains with the normal of the basal plane perpendicular to the loading direction.

4. Discussion

4.1 Texture vs random orientation of grains

It has been believed that extruded magnesium alloy has a crystallographic texture whose *c*-axis in most grains is perpendicular to the extruded direction. By loading in the extruded direction of a specimen whose surface layer was removed to obtain a sound specimen surface, we found that twinning and detwinning occurred under compressive and tensile stresses, respectively [5]. We also confirmed such behavior by EBSD analysis, as shown in Figs. 4 and 5, revealing that twin bands are formed not under tensile stress but under compressive stress, and these twin bands disappeared after the following application of tensile stress owing to detwinning. Figure 5 shows that (a) there were no twin bands in the as-received material, (b) the twin bands shown by arrows were formed upon the first application of compressive stress, (c) all twin bands disappeared under the following application of tensile stress owing to detwinning, and (d) with the second application of compression stress, twin bands formed by the first application of compressive stress, indicated by downward arrows in (b), appeared again in the second application of compressive stress (d). In contrast, a twin band formed by the first application of compressive stress, indicated by the right-pointing arrow in (b), never formed with the second application of compressive stress (d). The twin bands indicated by left-pointing arrows in (d) were formed by the second application of compression stress; these were not observed after the first application of compressive stress (b), indicating that not all twin bands persisted and new twin bands are formed with every application of compression stress under cyclic loading [6], and the twinning–detwinning behavior must occur continuously but not for all twins.

As mentioned in the previous section, the orientation of grains in the surface layer of an extruded plate is not textured but random. Most engineering components and structures are employed in the as-extruded state and have crystallographically randomly orientated grains at the surface, where cracks are usually initiated. However, the twinning–detwinning behavior in a random-orientation grain structure has not been reported in previous studies. On the other hand, the twinning–detwinning behavior is different in a textured structure, as shown in Fig. 6, where twinning occurs not only under compression stress, but also under tensile stress, and most of the twin bands, formed under compression stress, are not detwinned by the following application of tensile stress.

4.2 Compression–compression fatigue

The twinning–detwinning behavior has been studied for fully reversed low-cycle fatigue and is believed to play an important role in the fatigue crack initiation mechanism. The fatigue crack initiation mechanism under compression–compression fatigue should be different from that under fully reversed low-cycle fatigue because the detwinning does not occur during compression–compression fatigue, and the orientation of the *c*-axis of most grains changes under compression–compression fatigue as shown in Fig. 7 but not under fully reversed fatigue. Although this finding was obtained for a specimen with randomly orientated grains at the surface, similar results should be obtained for specimens with textured surfaces under compression–compression fatigue because the random orientation can rotate to become textured resulting from the change in the orientation of grains owing to the repetition of twinning under the cyclic application of compressive stress without the detwinning due to application of tensile stress. This is different from the result obtained in fully reversed cyclic loading, $R = -1$, where the tensile and compressive stresses are applied cyclically. The mechanism is considered to be similar to that during the extrusion process, where the *c*-axis is directed along the compression direction to form texture [23].

For magnesium alloy under fully reversed high-cycle fatigue, the authors reported that fatigue cracks are formed from large grains with a high Schmid factor of the basal slip system, and that the crack initiation is a result of irreversible slipping that is unrelated to twinning, whereas cracks are initiated along grain boundaries with large misfit under compression–compression fatigue. For fully reversed high-cycle fatigue, Type A specimens with textured surfaces were employed, while Type C specimens with randomly orientated grains at the surface were employed for compression–compression fatigue. However, this difference in grain orientation is not responsible for the

difference in crack initiation mechanism because the orientation of grains around the crack initiation site under compression–compression fatigue shown in Fig. 8 is similar to that in Type A specimens, *i.e.*, the direction of the *c*-axis of grains is normal to the specimen surface. It is still unclear why the detwinning mechanism is not in effect after the application of tensile stress shown in Fig. 8（b). The orientation of the twin band differs from that shown in Figs. 4 and 5, although the orientations of mother crystals are similar.

5. Conclusions

To elucidate the fatigue crack initiation mechanism, several types of cyclic stress were applied to specimens made of an extruded magnesium alloy, AZ31, and the twinning, detwinning, and fatigue crack initiation behaviors were investigated by EBSD analysis. The following results were obtained.

1. The crystallographic orientation of the extruded AZ31 plate is random at the surface whereas it has texture with the normal of the basal plane perpendicular to the surface at 300 μm beneath the surface.
2. In both texture and random orientation, twinning occurred under compressive stress exceeding the compressive yield strength. Detwinning occurred only in the texture region, and the twin bands disappeared following the application of tensile stress smaller than the yield strength of monotonic loading, whereas detwinning did not occur in the random-orientation material.
3. In compression–compression fatigue test, twinning occurred. As a result of successive twinning, the random orientation of grains changed to a texture in which the *c*-axis is parallel to the loading direction.
4. In compression–compression fatigue test, cracks were formed along the boundary of grains with a high Schmid factor of the basal slip system and the misfit between the grains on the two sides is large. Near the crack initiation site, twin bands were observed, and detwinning did not occur under the tensile stress after compression–compression cyclic loading.

Acknowledgement

Support of this work through a Grant-in-Aid for Scientific Research (C) from Japan Society for the Promotion of Science under proposal number 18K03837 (Head investigator: Professor Y. Nakai, Kobe University) is gratefully acknowledged. The authors would like to thank Dr. Yuki Nakamura (National Institute of Technology, Toyota College) for their experimental support.

References

[1] L. Wu, A. Jain, D.W. Brown, G.M. Stoica, S.R. Agnew, B. Clausen, D.E. Fielden, P.K. Liaw, Twinning-detwinning behavior during the strain-controlled low-cycle fatigue testing of a wrought magnesium alloy, ZK60A, Acta Mater.: 56 (2008) 688-695.

[2] L. Wu, S.R. Agnew, D.W. Brown, G.W. Stoica, B. Clausen, A. Jain, D.E. Fielden, P.K. Liaw, Internal stress relaxation and load redistribution during the twinning–detwinning-dominated cyclic deformation of a wrought magnesium alloy, ZK60A, Acta Mater.: 56 (2008) 3699-3707.

[3] Y. Nakai, M. Saka, H. Yoshida, K. Asayama, S. Kikuchi, Fatigue crack initiation site and propagation paths in high-cycle fatigue of magnesium alloy AZ31, Int. J. Fatigue: 123 (2019) 248-254.

[4] Y. Nakai, D. Shiozawa, S. Kikuchi, Y. Nakagawa, K. Asayama, Observations of twinning and detwinning in magnesium alloy by synchrotron radiation DCT and EBSD, Struct. Integ. Procedia: 2 (2019) 83-88.

[5] Y. Nakai, S. Kikuchi, K. Asayama, H. Yoshida, Stress ratio effect on fatigue crack initiation mechanism of magnesium alloy AZ31, Mater. Sci. Forum: 1016 (2021) 1003-1008.

[6] A.D. Murphy-Leonard, D.C. Pagan, A. Beaudoin, M.P. Miller, J.E. Allison, Quantification of cyclic twinning-detwinning behavior during low-cycle fatigue of pure magnesium using high energy X-ray diffraction, Int. J. Fatigue, (2019) 314-323.

[7] K. Shiozawa, T. Kashiwagi, T. Murai, T. Takahashi, Gigacycle fatigue behavior and fractography of extruded AZ80 magnesium alloy, Trans. Jpn Soc. Mech. Eng. A: 75 (2009) 733-741.

[8] S. Begum, D.L. Chen, S. Xu, A.A. Luo, Effect of strain ratio and strain rate on low cycle fatigue behavior of AZ31 wrought magnesium alloy, Mat. Sci. Eng. A: 517 (25009) 334-343.

[9] M. Matsuzuki, S. Horibe, Analysis of fatigue damage process in magnesium alloy AZ31, Mater. Sci. Eng. A: 504 (2009) 169-174.

[10] K. Tanaka, Y. Nakai, O. Maekawa, Microscopic study on fatigue crack initiation and early propagation in smooth specimen of low carbon steel, J. Soc. Mater. Sci. Jpn: 31 (1982) 376-382.

[11] Y. Nakai, S. Fukuhara, K. Ohnishi,. Observation of fatigue damage in structural steel by scanning atomic-force microscopy, Int. J. Fatigue: 19 (1997) S223-S36.

[12] Y. Nakai, T. Kusukawa, N. Hayashi, Scanning atomic-force microscopy on initiation and growth behavior of fatigue slip-bands in α-brass, ASTM STP: 1406 (2002) 122-135.

[13] Z.Y. Nan, S. Ishihara, T. Goshima, R. Nakanishi, Scanning probe microscope observations of fatigue process in magnesium alloy AZ31 near the fatigue limit, Scripta Meter.: 50 (2004) 429-434.

[14] M. Kamakura, K. Tokaji, Y. Ishizumi, N. Hasegawa, Fatigue behavior and fracture mechanism of an extruded AZ61 magnesium alloy, J. Soc. Mat. Sci. Jpn: 53 (2004) 1371-1377.

[15] F. Yang, S.M. Yin, S.X. Li, Z.F. Zhang, Crack initiation mechanism of extruded AZ31 magnesium alloy in the very high cycle fatigue regime, Mater. Sci. Eng. A: 491 (2008) 131-136.

[16] Y. Uematsu, T. Sugie, Effect of grain orientation on small fatigue crack growth behavior in magnesium alloy AZ31 rolled plate, Trans. Jpn Soc. Mech. Eng. A: 76 (2010) 311-316.

[17] L. Nascimento, S.Y.J. Bohlen, L. Fuskova, D. Letzig, K.U. Kainer, High cycle fatigue behavior of magnesium alloys, Proc. Eng.: 2 (2010) 743-750.

[18] A. King, W. Ludwig, M. Herbig, J.Y. Buffiére, A.A. Khan, Three-dimensional in situ observations of short fatigue crack growth in magnesium, Acta Mater.: 59 (2011) 6761-671.

[19] Y. Uematsu, T. Kakiuchi, K. Tamada, Y. Kimia, EBSD analysis of fatigue crack initiation behavior in coarse-grained AZ31 magnesium alloy, Int. J. Fatigue: 84 (2016) 1-8.

[20] T. Tokaji, M. Kamakura, Y. Ishizumi, N. Hasegawa, Fatigue behavior and fracture mechanism of a rolled AZ31 magnesium alloy, Int. J. Fatigue: 26 (2004) 1217-1224.

[21] Y. Ochi, K. Masaki, T. Hirasawa, X. Wu, T. Matsumura, Y. Takigawa, K. Higashi, High cycle fatigue property and micro crack propagation behavior in extruded AZ31 magnesium alloys, Mater. Trans.: 47 (2006) 989-994.

[22] T. Sakai, S. Kikuchi, Y. Nakamura, N. Ninomiya, A study on very high cycle fatigue properties of low flammability magnesium alloy in rotating bending and axial loading, Appl. Mech. Mater.: 782 (2015) 27-41.

[23] A. Styczynski, Ch. Hartig, J. Bohlen, D. Letzig, Cold rolling textures in AZ31 wrought magnesium alloy, Scripta Mater.: 50 (2004) 943-947.

[24] M.J Philippe, Texture formation in hexagonal materials, Mater Sci Forum: 57-162 (1994) 1337-1350, 1994.

[25] H. Neuber, Kerbspannungslehre Zweite Auflage. Springer-Verlag (1958) p.84.

[26] K. Tanaka and Y. Nakai, Prediction of Fatigue Threshold of Notched Components, J Eng Mater Tech, Trans ASME, 106 (1984) 192-199.

List of Tables and Figures

by right-pointing arrow in (a) do not appear in (d), and twin bands indicated by left-pointing arrows in (d) are not formed in (a), and twin bands indicated by downward arrows can be observed both in (b) and (d).

Fig. 8. Orientation of grains on Side A specimen surface after start of cyclic loading with compression for Type B specimen with orientation of grains are random distributed at surface). Twin bands indicated by downward arrows can be observed both in (a) and (b), those indicated by right-pointing arrows in (a) disappeared in (b), and left-pointing arrow indicate $[10\bar{1}2]$ twin bands appeared in (b) cannot be observed in (a).

Fig. 9. Orientation of grains on Side A specimen surface at $N = 1.0\times10^7$ cycles under compression–compression fatigue with the maximum and minimum stresses are -14 and -140 MPa, respectively (Type C specimen with random orientation surface). At this number of cycles, fatigue cracks are already initiated but do not propagate. Arrows indicate twin bands.

Fig. 10. Orientation and Schmid factor of grains on Side A specimen surface at $N = 1.0\times10^7$ cycles under compression–compression fatigue after crack initiation (Type C specimen with random orientation surface) [5]. Arrows indicate twin bands.

Figure(s) Click here to access/download;Figure(s);Mg2-Table-Figure Rev6.docx

Table 1. Chemical composition of AZ31 (mass %).

Al	Zn	Mn	Fe	Ni	Cu	Si	Mg
2.7	0.79	0.44	0.0012	0.009	0.011	0.004	bal.

Table 2. Average grain size and mechanical properties.

Average grain size (μm)	Tensile yield strength (MPa)	Compressive yield strength (MPa)
52	286	79

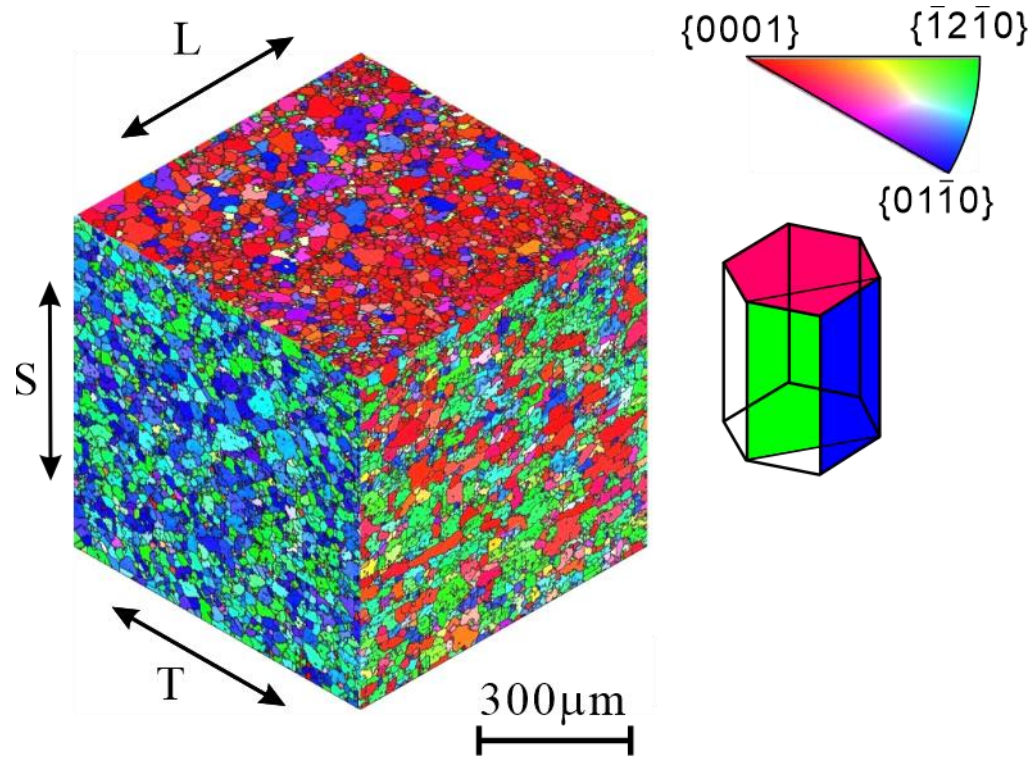

Figure 1. Microstructure near the midsection of as-received plate where colors indicate orientation of grains normal to each plane [3].

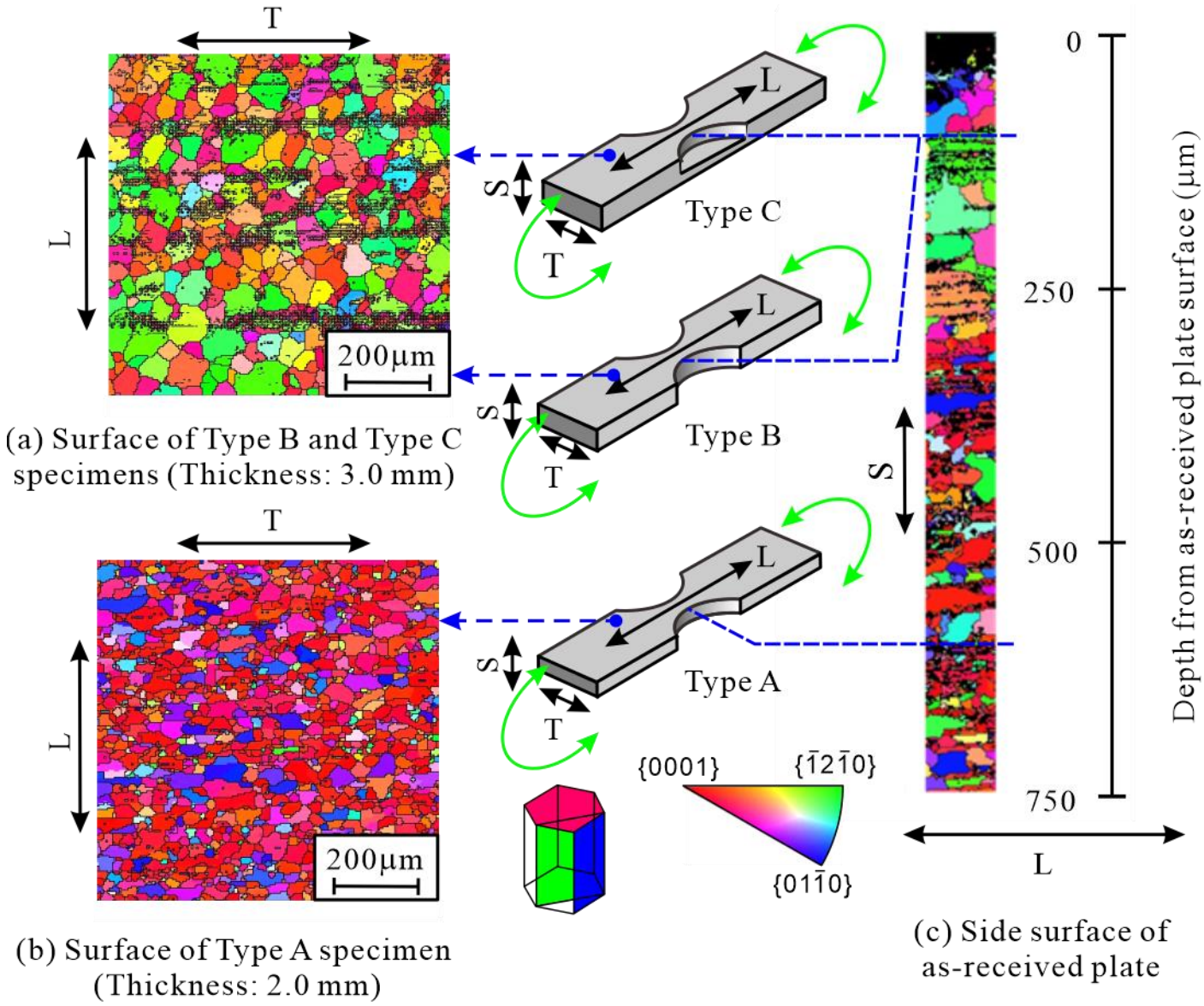

Figure 2. Crystallographic orientation of grains in S-direction, where grains in the surface shown in (a) are random distributed and those are textured in (b).

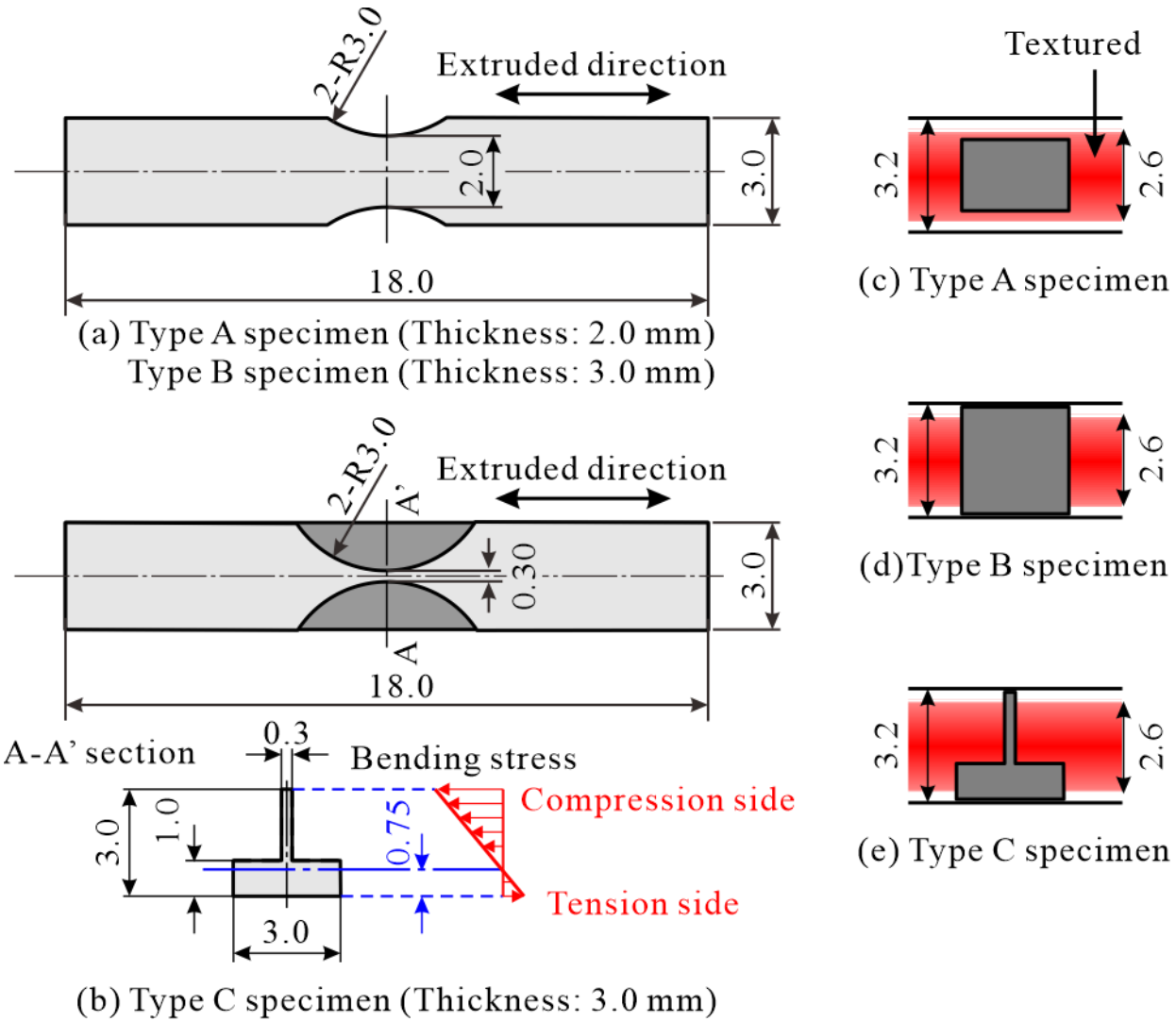

Figure 3. Types of specimens (Dimensions in mm) , where Type A and Type B specimens were employed for the observations of the initial few cycles, and Type C specimen for compression–compression fatigue tests, respectively. Cross-sections of as-received plate and specimens are indicated from (c) to (e).

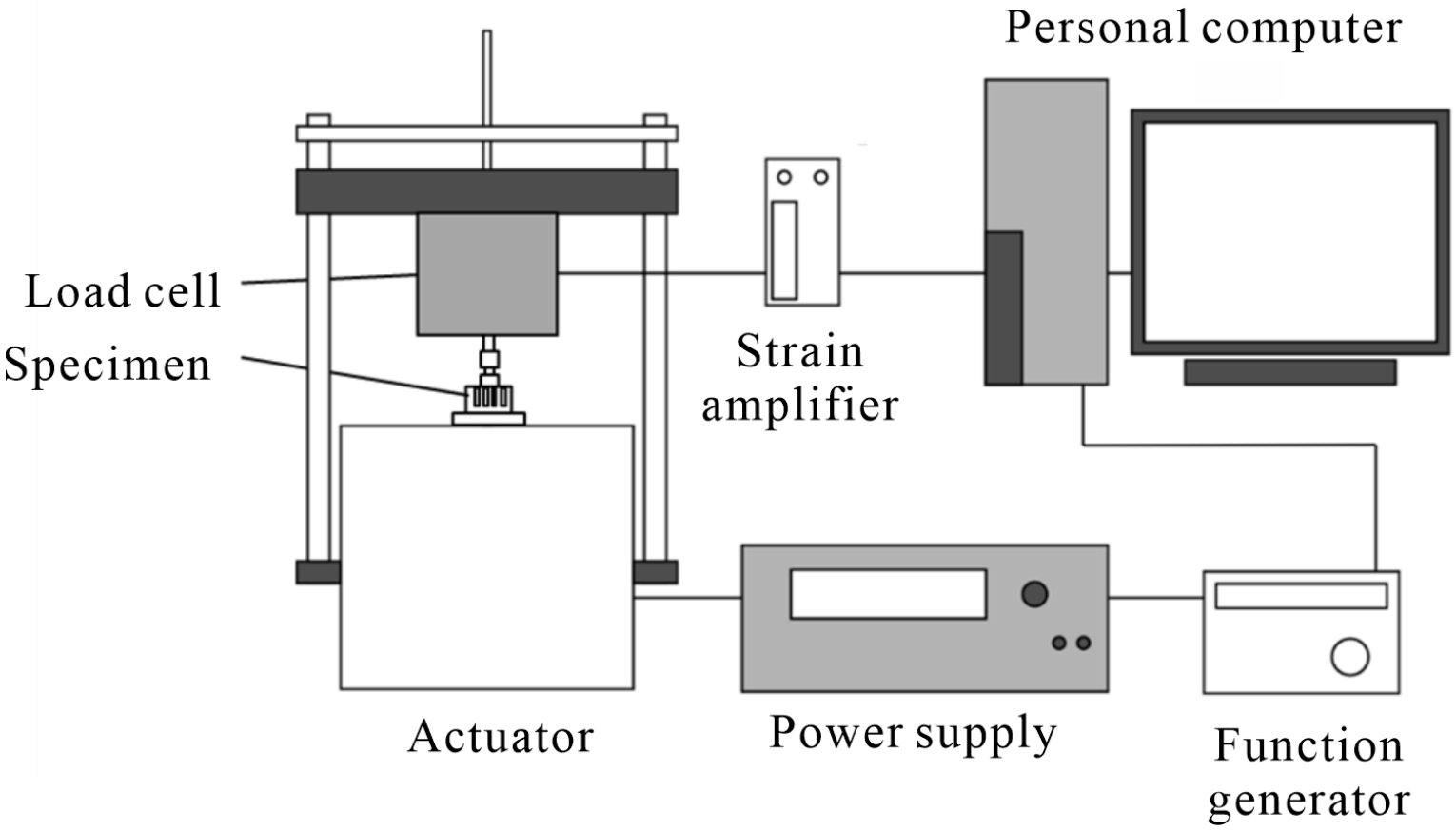

Figure 4 Configuration of fatigue test system.

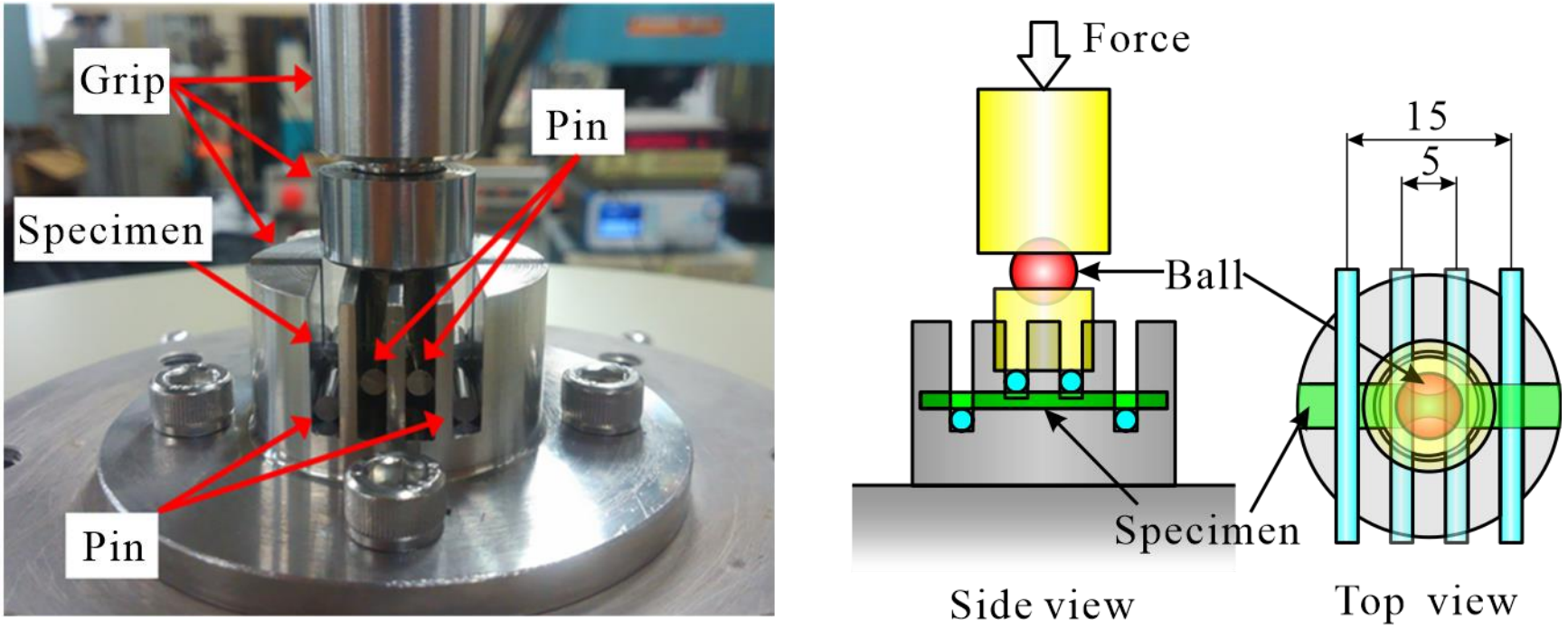

Figure 5 Appearance of loading device of four-point bending.

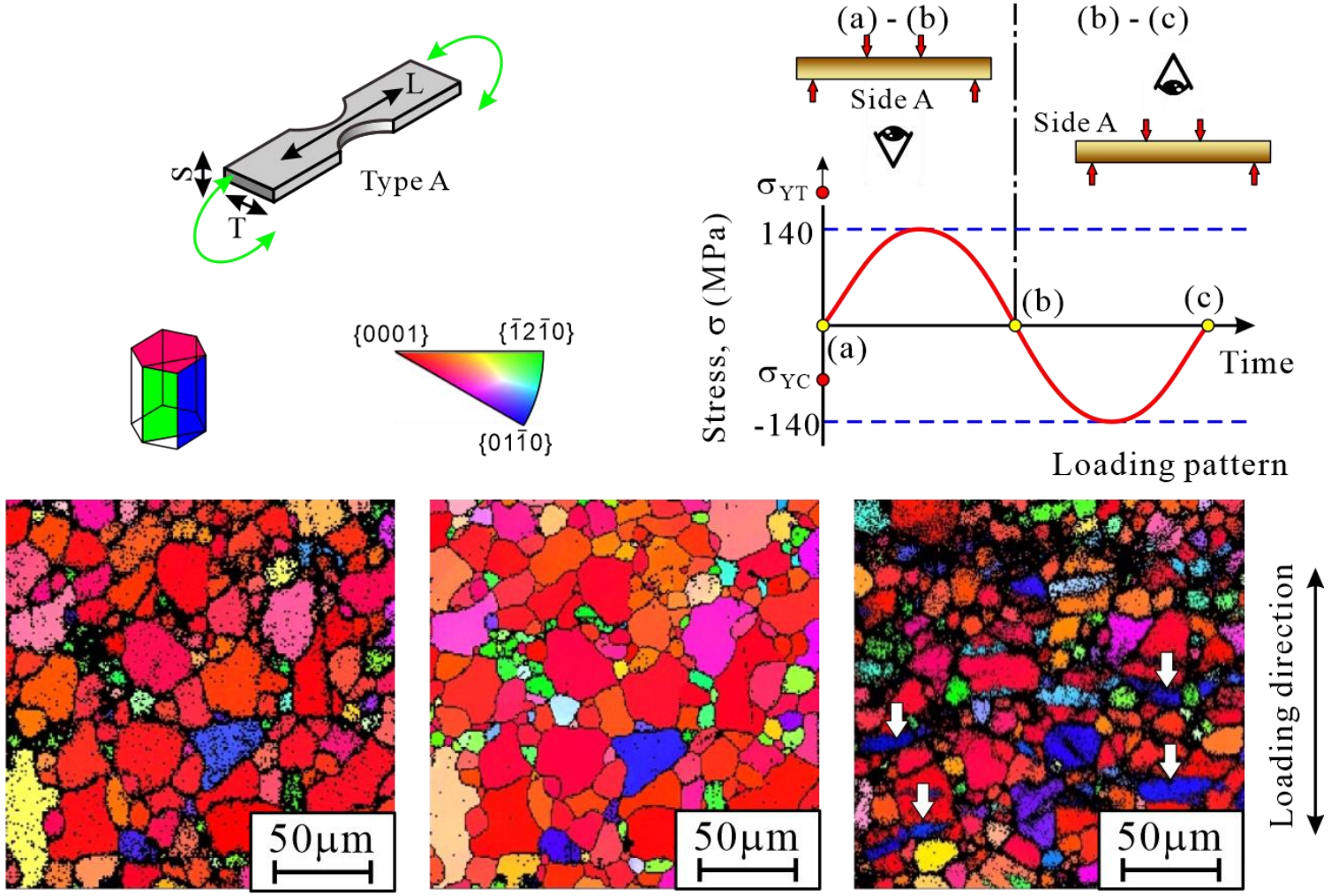

Figure 6. Orientation of grains on Side A specimen surface after cyclic loading start with tension for Type A specimen which exhibits texture surface, where the maximum tensile stress was less than the tensile yield strength σ_{YT}, and the maximum compressive stress (absolute value) exceeded the compressive yield strength σ_{YC} under monotonic loading. Arrows indicated in (c) are $[10\bar{1}1]$ twin bands.

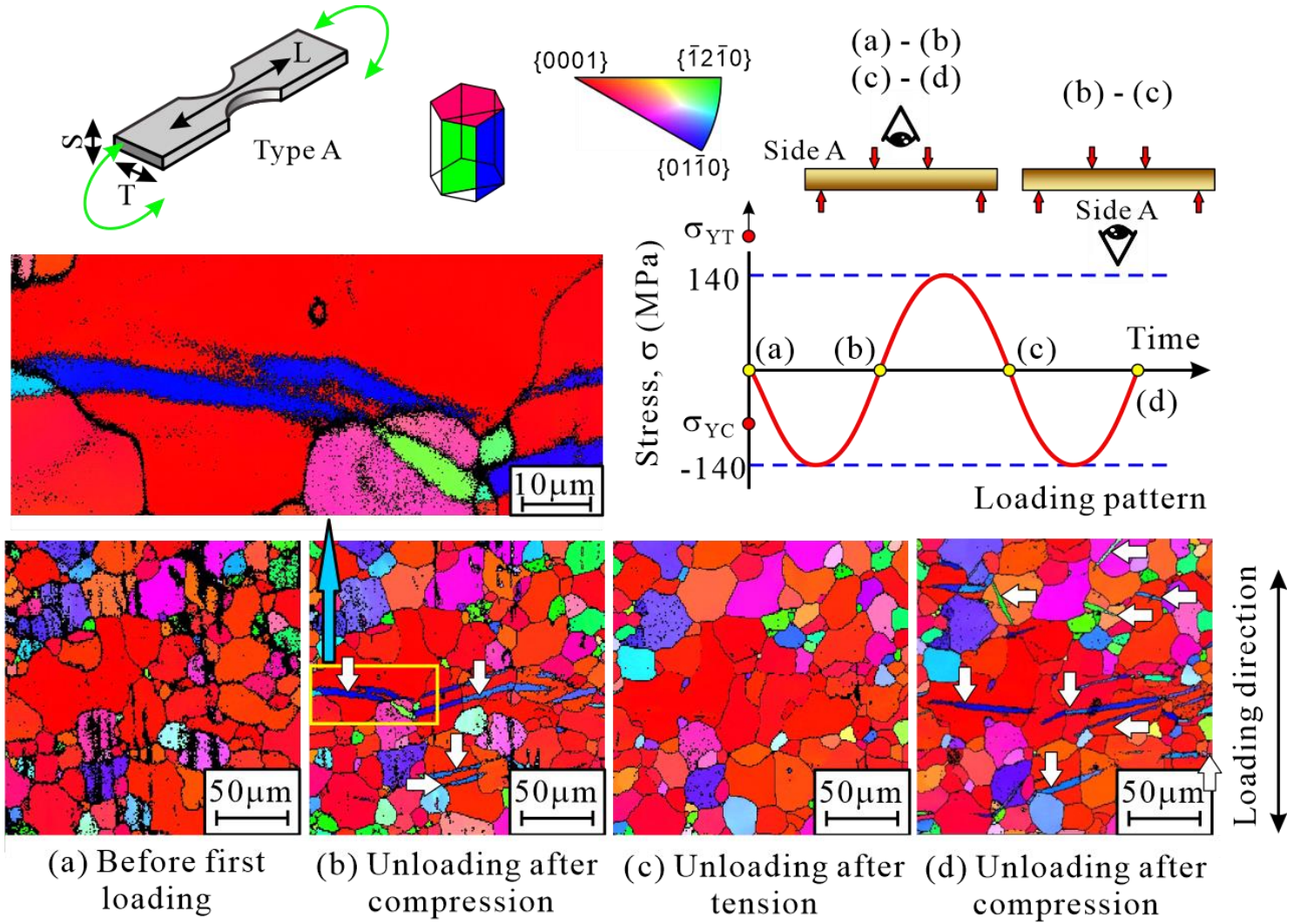

Figure 7. Orientation of grains on Side A specimen surface after start of cyclic loading with compression for Type A which has texture surface, where the maximum compressive stress (absolute value) exceeded the compressive yield strength σ_{YC}, and maximum tensile stress was less than the tensile yield strength σ_{YT} under monotonic loading. A twin band indicated by right-pointing arrow in (a) do not appear in (d), and twin bands indicated by left-pointing arrows in (d) are not formed in (a), and twin bands indicated by downward arrows can be observed both in (b) and (d).

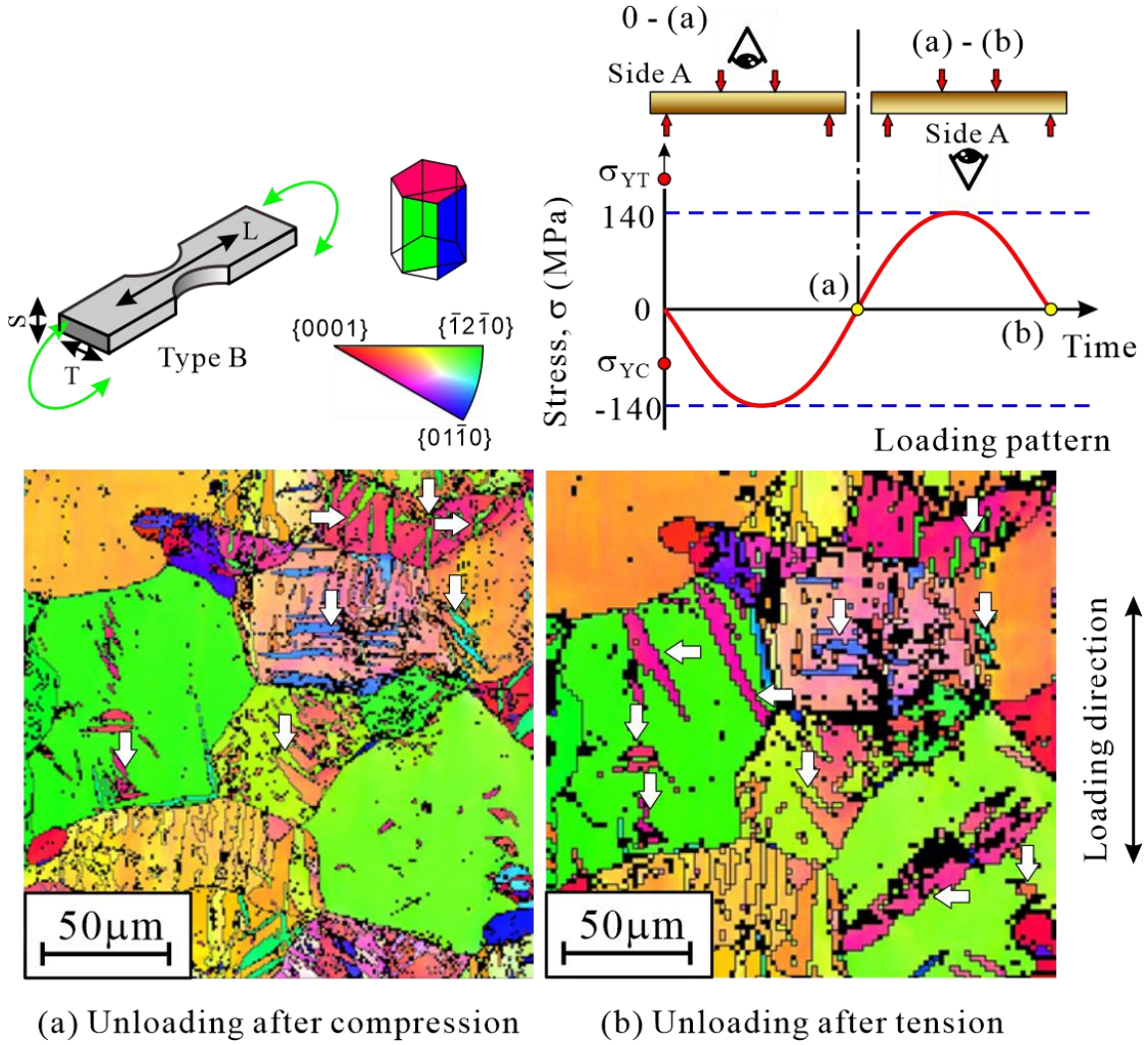

Figure 8. Orientation of grains on Side A specimen surface after start of cyclic loading with compression for Type B specimen with orientation of grains are random distributed at surface). Twin bands indicated by downward arrows can be observed both in (a) and (b), those indicated by right-pointing arrows in (a) disappeared in (b), and left-pointing arrow indicate $[10\bar{1}2]$ twin bands appeared in (b) cannot be observed in (a).

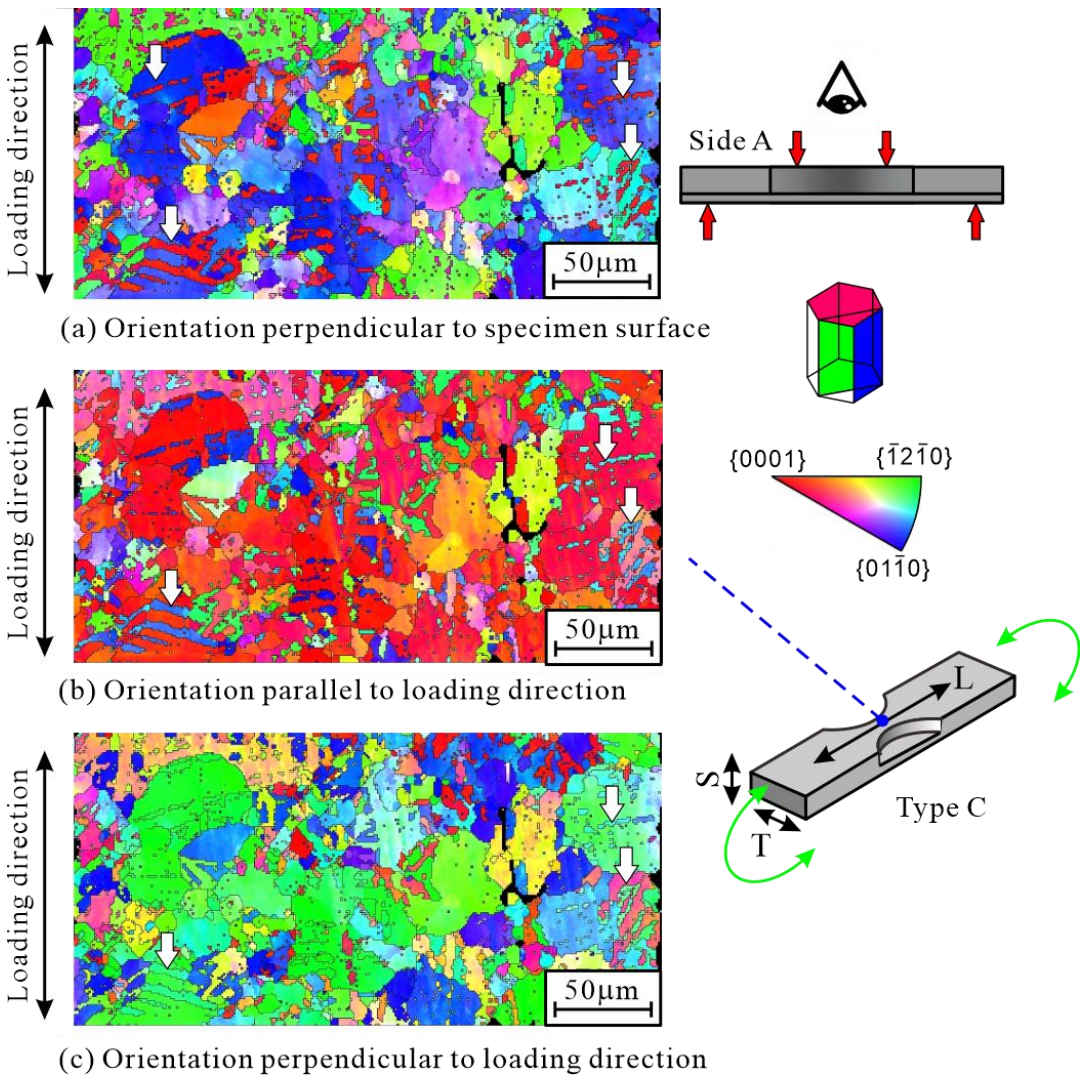

Figure 9. Orientation of grains on Side A specimen surface at N = 1.0×10^7 cycles under compression–compression fatigue with the maximum and minimum stresses are -14 and -140 MPa, respectively (Type C specimen with random orientation surface). At this number of cycles, fatigue cracks are already initiated but do not propagate. Arrows indicate twin bands.

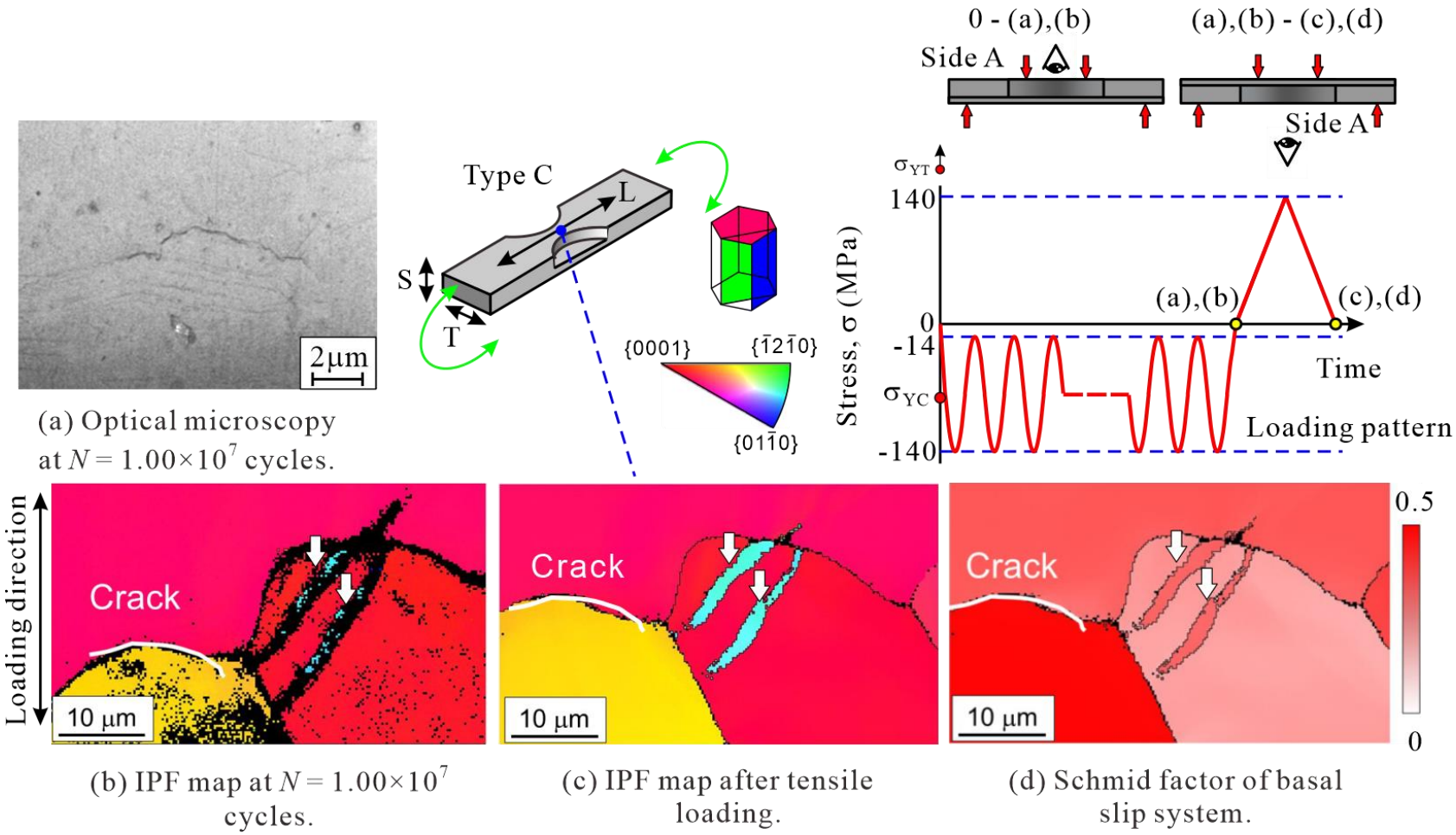

Figure 10. Orientation and Schmid factor of grains on Side A specimen surface at $N = 1.0\times10^7$ cycles under compression–compression fatigue after crack initiation (Type C specimen with random orientation surface) [5]. Arrows indicate twin bands.